**Advances in Materials Research**, *Vol. 5, No. 1 (2016) 35-53*
DOI: http://dx.doi.org/10.12989/amr.2016.5.1.035 

# Bending analysis of an imperfect FGM plates under hygro-thermo-mechanical loading with analytical validation

Tahar Hassaine Daouadji[1,2*], Belkacem Adim[1,2] and Rabia Benferhat[3]

[1]*Département de génie civil , Université Ibn Khaldoun Tiaret; BP 78 Zaaroura, 14000 Tiaret, Algérie.*
[2]*Laboratoire de Géomatique et Développement Durable, Université Ibn Khaldoun de Tiaret Algérie.*
[3]*Laboratoire de Géomatériaux , Département de Génie Civil, Université de Chlef, Algérie.*

*(Received April 11, 2016, Revised June 20, 2016, Accepted June 21, 2016)*

**Abstract.** Flexural bending analysis of perfect and imperfect functionally graded materials plates under hygro-thermo-mechanical loading are investigated in this present paper. Due to technical problems during FGM fabrication, porosities and micro-voids can be created inside FGM samples which may lead to the reduction in density and strength of materials. In this investigation, the FGM plates are assumed to have even and uneven distributions of porosities over the plate cross-section. The modified rule of mixture is used to approximate material properties of the FGM plates including the porosity volume fraction. In order the elastic coefficients, thermal coefficient and moisture expansion coefficient of the plate are assumed to be graded in the thickness direction. The elastic foundation is modeled as two-parameter Pasternak foundation. The equilibrium equations are given and a number of examples are solved to illustrate bending response of Metal-Ceramic plates subjected to hygro-thermo-mechanical effects and resting on elastic foundations. The influences played by many parameters are investigated.

**Keywords:** FGM plate; moisture concentration; thermal field; elastic foundations; higher-order shear deformation theory

## 1. Introduction

Functionally graded materials(FGMs), possessing spatially varying properties, have been developed for special components such as rocket engine components, aerospace structures, etc. The earliest FGMs were introduced by Japanese scientists in the mid 1980 as ultra-high temperature resistant materials for aerospace applications. Recently, these materials have found other uses in electrical devices, energy transformation, biomedical engineering, optics, etc (Suresh ,1998). However, in FGM fabrication, micro voids or porosities can occur within the materials during the process of sintering. This is because of the large difference in solidification temperatures between material constituents (Zhu 2001). Wattanasakulpong (2012) also gave the discussion on porosities happening inside FGM samples fabricated by a multi-step sequential infiltration technique. Therefore, it is important to take into account the porosity effect when designing FGM structures subjected to dynamic loadings. The degradation in performance of the

*Corresponding author, Ph.D., E-mail: daouadjitah@yahoo.fr


http://www.techno-press.org/?journal=amr&subpage=7 ISSN: 2234-0912 (Print), 2234-179X (Online)

structure due to moisture concentration and high temperature has become increasingly more important with the prolonged use of functionally graded materials (FGMs) in many structural applications. As a result, hygrothermal internal stresses are generated with the change of environment. These stresses generally induce large deformation and could even contribute to the failure of the structure. The deformation and stress analysis of different plate structures subjected to moisture and temperature has been the subject of research interest of many investigators (Patel *et al.* 2002, Bahrami *et al.* 2007, Benkhedda *et al.* 2008, Ait amar *et al.* 2014, Benoun *et al.* 2016 and Bourada *et al.* 2015). The plates supported by an elastic foundation are very common in structural engineering. Many linear bending studies for thick plates subjected to transverse loads with elastic foundations are available in the literature (Voyiadjis *et al.* 1986). In some of the analyses of plates on elastic foundation, a single parameter is used to describe the foundation behavior according to Winkler's model (Liu 2000).

Based on the open literature, it is found that many researchers have paid their attention on investigating the mechanical or the thermal or the thermo-mechanical responses of FG plates and shells. A comprehensive review is done by Tanigawa (1995). Reddy (2000) has analyzed the static behavior of functionally graded rectangular plates based on his third-order shear deformation plate theory. The static response of FG plate has been investigated by Zenkour (2006) using a generalized shear deformation theory. In a recent study, a new four variable refined plate theory which involves only four unknown functions and yet takes into account shear deformations has been developed (Benachour *et al.* 2011, Hassaine Daouadji 2012 and 2013, Tlidji *et al.* 2014, Benferhat *et al.* 2014, Abdelhak *et al.* 2015, Bouderba *et al.* 2013, Habali *et al.* 2014, Mahi *et al.* 2015, Ait yahia *et al.* 2015, Tounsi 2013, Bellifa 2015, Belabed 2014, Hamidi 2015 and Zidi *et al.* 2014). This four variable refined plate theory is based on the assumption that the in-plane and transverse displacements consist of bending and shear components in which the bending components do not contribute toward shear forces and, likewise, the shear components do not contribute toward bending moments. The most interesting feature of this theory is that it accounts for a quadratic variation of the transverse shear strains across the thickness, and satisfies the zero traction boundary conditions on the top and bottom surfaces of the plate without using shear correction factors. In addition, it has strong similarities with the classical plate theory in some aspects including the structure of the governing equation, boundary conditions and moment expressions.

In this study, is to extend the four variable refined plate theory to the hygro-thermo-mechanical bending behavior of perfect and imperfect FGM plate resting on elastic foundations, motivated by rocket-launch pad structural foundations under thermal propulsion loads. Some other researchers have modeled the foundation with two parameters according to Pasternak's model. This two-parameter model takes into account the effect of shear interaction among the points in the foundation (Shen 1999, zenkour 2009). The objective of this investigation is to present a general hygrothermal formulation for imperfect FGM plates resting on an elastic foundation using the sinusoidal shear deformation theory.

## 2. Mathematical model and governing equations

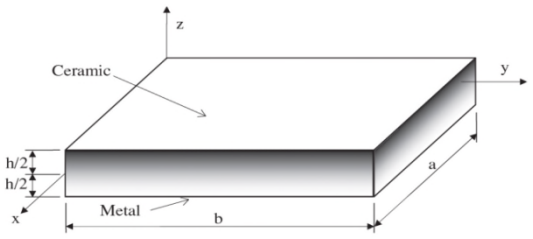


Fig. 1 Geometry of FGM rectangular plate

Consider a plate of total thickness $h$ and composed of imperfect functionally graded material through the thickness (Fig. 1). It is assumed that the material is isotropic and grading is assumed to be only through the thickness. The $xy$ plane is taken to be the undeformed mid plane of the plate with the $z$ axis positive upward from the mid plane.

### *2.1 Displacement fields and strains*

The assumed displacement field is as follows

$$\begin{aligned} u(x,y,z) &= u_0(x,y) - z\frac{\partial w_b}{\partial x} - (z - \sin(\frac{\pi z}{h}))\frac{\partial w_s}{\partial x} \\ v(x,y,z) &= v_0(x,y) - z\frac{\partial w_b}{\partial y} - (z - \sin(\frac{\pi z}{h}))\frac{\partial w_s}{\partial y} \\ w(x,y,z) &= w_b(x,y) + w_s(x,y) \end{aligned} \tag{1a}$$

where $\boldsymbol{u}_0$ and $\boldsymbol{v}_0$ are the mid-plane displacements of the plate in the $\boldsymbol{x}$ and $\boldsymbol{y}$ direction, respectively; $\boldsymbol{w}_b$ and $\boldsymbol{w}_s$ are the bending and shear components of transverse displacement, respectively, while $\boldsymbol{f}(z)$ represents shape functions determining the distribution of the transverse shear strains and stresses along the thickness (Benferhat *et al.* 2014) and is given as

$$f(z) = z - \sin(\frac{\pi z}{h}) \tag{1b}$$

It should be noted that unlike the first-order shear deformation theory, this theory does not require shear correction factors. The kinematic relations can be obtained as follows

$$\begin{aligned} \boldsymbol{\varepsilon}_x &= \boldsymbol{\varepsilon}_x^0 + z\,\boldsymbol{k}_x^b + \boldsymbol{f}(z)\,\boldsymbol{k}_x^s \\ \boldsymbol{\varepsilon}_y &= \boldsymbol{\varepsilon}_y^0 + z\,\boldsymbol{k}_y^b + \boldsymbol{f}(z)\,\boldsymbol{k}_y^s \\ \boldsymbol{\gamma}_{xy} &= \boldsymbol{\gamma}_{xy}^0 + z\,\boldsymbol{k}_{xy}^b + \boldsymbol{f}(z)\,\boldsymbol{k}_{xy}^s \\ \boldsymbol{\gamma}_{yz} &= \boldsymbol{g}(z)\,\boldsymbol{\gamma}_{yz}^s \\ \boldsymbol{\gamma}_{xz} &= \boldsymbol{g}(z)\,\boldsymbol{\gamma}_{xz}^s \\ \boldsymbol{\varepsilon}_z &= 0 \end{aligned} \tag{2}$$

where

$$\boldsymbol{\varepsilon}_x^0 = \frac{\partial \boldsymbol{u}_0}{\partial \boldsymbol{x}}, \quad \boldsymbol{k}_x^b = -\frac{\partial^2 \boldsymbol{w}_b}{\partial \boldsymbol{x}^2}, \quad \boldsymbol{k}_x^s = -\frac{\partial^2 \boldsymbol{w}_s}{\partial \boldsymbol{x}^2}, \quad \boldsymbol{\varepsilon}_y^0 = \frac{\partial \boldsymbol{v}_0}{\partial \boldsymbol{y}}, \quad \boldsymbol{k}_y^b = -\frac{\partial^2 \boldsymbol{w}_b}{\partial \boldsymbol{y}^2}, \quad \boldsymbol{k}_y^s = -\frac{\partial^2 \boldsymbol{w}_s}{\partial \boldsymbol{y}^2}, \quad \boldsymbol{\gamma}_{xy}^0 = \frac{\partial \boldsymbol{u}_0}{\partial \boldsymbol{y}} + \frac{\partial \boldsymbol{v}_0}{\partial \boldsymbol{x}}, \tag{3}$$

$$k_{xy}^{b}=-2\frac{\partial^2 w_b}{\partial x\partial y},\quad k_{xy}^{s}=-2\frac{\partial^2 w_s}{\partial x\partial y},\quad \gamma_{yz}^{s}=\frac{\partial w_s}{\partial y},\quad \gamma_{xz}^{s}=\frac{\partial w_s}{\partial x},\quad g(z)=1-f'(z)\ \text{ and }\ f'(z)=\frac{df(z)}{dz}$$

### 2.2 Constitutive equations

Consider a rectangular plate of length *a*, width *b* and thickness *h* made of imperfect functionally graded material. The plate is graded from metal to ceramic. The plate is subjected to a sinusoidal distributed load *q(x,y)* and a temperature field *T(x, y, z)* as well as a moisture concentration *C(x, y, z)*. The material properties *V(z)* of the FGM plate, such as Young's modulus $E$ , Poisson's ratio $\nu$ , and thermal $\alpha$ and moisture expansion $\beta$ coefficients are given according to the modified rule of mixture as

$$V(z)=V_m+(V_c-V_m)\left(\frac{1}{2}+\frac{z}{h}\right)^{p}-(V_c+V_m)\frac{\zeta}{2} \tag{4}$$

Where $V_c$ and $V_m$ are the corresponding properties of the ceramic and metal, respectively, and $\boldsymbol{p}$ is the volume fraction exponent which takes values greater than or equal to zero, and $\zeta$ is the porosity volume fraction of the imperfect FGM plate ($\zeta$ <<1) sited in (Wattanasakulpong 2012), perfect FGM plate can be obtained by setting $\zeta$ =0. The linear constitutive relations are

$$\begin{Bmatrix}\sigma_x\\ \sigma_y\\ \tau_{xy}\end{Bmatrix}=\begin{bmatrix}Q_{11} & Q_{12} & 0\\ Q_{12} & Q_{22} & 0\\ 0 & 0 & Q_{66}\end{bmatrix}\begin{Bmatrix}\varepsilon_x-\alpha\Delta T-\beta\Delta C\\ \varepsilon_y-\alpha\Delta T-\beta\Delta C\\ \gamma_{xy}\end{Bmatrix}$$
$$\begin{Bmatrix}\tau_{yz}\\ \tau_{zx}\end{Bmatrix}=\begin{bmatrix}Q_{44} & 0\\ 0 & Q_{55}\end{bmatrix}\begin{Bmatrix}\gamma_{yz}\\ \gamma_{zx}\end{Bmatrix} \tag{5}$$

Where $(\sigma_x,\sigma_y,\tau_{yz},\tau_{xz},\tau_{xy})$ and $(\varepsilon_x,\varepsilon_y,\gamma_{yz},\gamma_{xz},\gamma_{xy})$ are the stress and strain components, respectively. Using the material properties defined in Eq. (4), stiffness coefficients, $\boldsymbol{Q_{ij}}$, can be expressed as

$$Q_{11}=Q_{22}=\frac{E(z)}{1-\nu^2}\quad Q_{12}=\frac{\nu E(z)}{1-\nu^2}\qquad Q_{44}=Q_{55}=Q_{66}=\frac{E(z)}{2(1+\nu)} \tag{6}$$

Where $\Delta T = T - T_0$ and $\Delta C = C - C_0$ in which $T_0$ is the reference temperature and $C_0$ is the reference moisture concentration. Now, let us consider a temperature distribution field *T(x,y,z)* and the moisture concentration *C(x,y,z)* in the plate domain *V* (plate volume) in the form

$$T(x,y,z)=T_z(z)T_\Omega(x,y)\ ,\quad C(x,y,z)=C_z(z)C_\Omega(x,y) \tag{7a}$$

Where $T_z$ *(z)* and $C_z$ *(z)* represent the temperature and the moisture concentration profile across the plate thickness coordinate *z*, respectively, where as $T_\Omega$ *(x, y)* and $C_\Omega$ *(x, y)* are the temperature and the moisture concentration distributions, respectively, over the reference surface domain $\Omega$ . In the most general case, the form of $T_z$ *(z)* is a result of the solution of a heat conduction problem. This calculated $T_z$ *(z)* turns out to be a nonlinear polynomial of *z*, often of a transcendental form (Zenkour 2009). In the case of a thick multi-layered structure, $T_z$ *(z)* would may be require a layerwise description (Tlidji *et al.* 2014), that is: plate theories with higher-order (or layerwise) displacement fields are required to capture a temperature profile obtained from the solution of a

heat-conduction problem. In the present study, the moisture concentration *C(x,y,z)* and the temperature distribution field *T(x,y,z)* are given as (Tlidji *et al.* 2014)

$$T(x,y,z) = T_1(x,y) + \frac{z}{h}T_2(x,y) + \frac{1}{\pi}\sin\left(\frac{\pi z}{h}\right)T_3(x,y) \tag{7b}$$

$$C(x,y,z) = C_1(x,y) + \frac{z}{h}C_2(x,y) + \frac{1}{\pi}\sin\left(\frac{\pi z}{h}\right)C_3(x,y) \tag{7c}$$

### *2.3 Governing equations*

The governing equations of equilibrium can be derived by using the principle of virtual displacements. The principle of virtual work in the present case yields

$$\int_{-h/2}^{h/2}\int_{\Omega}\left[\sigma_x\delta\varepsilon_x + \sigma_y\delta\varepsilon_y + \tau_{xy}\delta\gamma_{xy} + \tau_{yz}\delta\gamma_{yz} + \tau_{xz}\delta\gamma_{xz}\right]d\Omega\,dz - \int_{\Omega}(q - f_e)\delta w dz = 0 \tag{8}$$

Where Ω is the top surface and $\boldsymbol{f_e}$ is the density of reaction force of foundation. For the Pasternak foundation model

$$f_e = K_w w - J_1\frac{\partial w}{\partial x^2} - J_2\frac{\partial w}{\partial y^2} \tag{9}$$

where $K_w$ is the modulus of subgrade reaction (elastic coefficient of the foundation) and $J_1$ and $J_2$ are the shear moduli of the subgrade (shear layer foundation stiffness). If the foundation is homogeneous and isotropic, this implies that $\boldsymbol{J_1 = J_2 = J_0}$. If the shear layer foundation stiffness is neglected, Pasternak foundation becomes a Winkler foundation.
Substituting Eqs. (2) and (5) into Eq. (8) and integrating through the thickness of the plate, Eq. (8) can be rewritten as

$$\begin{aligned}\int_{\Omega}\Big[&N_x\delta\varepsilon^0_x + N_y\delta\varepsilon^0_y + N_{xy}\delta\gamma^0_{xy} + M^b_x\delta k^b_x + M^b_y\delta k^b_y + M^b_{xy}\delta k^b_{xy} + M^s_x\delta k^s_x + M^s_y\delta k^s_y \\ &+ M^s_{xy}\delta k^s_{xy} + S^s_{yz}\delta\gamma^s_{yz} + S^s_{xz}\delta\gamma^s_{xz}\Big]d\Omega - \int_{\Omega}(q - f_e)(\delta w_b + \delta w_s)d\Omega = 0\end{aligned} \tag{10}$$

The stress resultants *N*, *M*, and *S* are defined by

$$\begin{Bmatrix} N_x & N_y & N_{xy} \\ M^b_x & M^b_y & M^b_{xy} \\ M^s_x & M^s_y & M^s_{xy} \end{Bmatrix} = \int_{-\frac{h}{2}}^{\frac{h}{2}}(\sigma_x,\sigma_y,\tau_{xy})\begin{Bmatrix} 1 \\ z \\ f(z) \end{Bmatrix}dz \tag{11a}$$

$$(S^s_{xz}, S^s_{yz}) = \int_{-\frac{h}{2}}^{\frac{h}{2}}(\tau_{xz},\tau_{yz})g(z)dz \tag{11b}$$

Substituting Eq. (5) into Eq. (11) and integrating through the thickness of the plate, the stress resultants are given as

$$\begin{Bmatrix} N \\ M^b \\ M^s \end{Bmatrix} = \begin{bmatrix} A & B & B^s \\ B & D & D^s \\ B^s & D^s & H^s \end{bmatrix}\begin{Bmatrix} \varepsilon \\ k^b \\ k^s \end{Bmatrix} - \begin{Bmatrix} N^T \\ M^{bT} \\ M^{sT} \end{Bmatrix} - \begin{Bmatrix} N^C \\ M^{bC} \\ M^{sC} \end{Bmatrix} \tag{12a}$$

$$\begin{Bmatrix} S^{\,s}_{yz} \\ S^{\,s}_{xz} \end{Bmatrix} = \begin{bmatrix} A^{s}_{44} & 0 \\ 0 & A^{s}_{55} \end{bmatrix} \begin{Bmatrix} \gamma^{\,s}_{yz} \\ \gamma^{\,s}_{xz} \end{Bmatrix} \tag{12b}$$

Where

$$N = \{N_x, N_y, N_{xy}\}^t, \quad M^b = \{M^b_x, M^b_y, M^b_{xy}\}^t, \quad M^s = \{M^s_x, M^s_y, M^s_{xy}\}^t \tag{13a}$$

$$N^T = \{N^T_x, N^T_y, 0\}^t, M^{bT} = \{M^{bT}_x, M^{bT}_y, 0\}^t, M^{sT} = \{M^{sT}_x, M^{sT}_y, 0\}^t \tag{13b}$$

$$N^C = \{N^C_x, N^C_y, 0\}^t, M^{bC} = \{M^{bC}_x, M^{bC}_y, 0\}^t, M^{sC} = \{M^{sC}_x, M^{sC}_y, 0\}^t \tag{13c}$$

$$\varepsilon = \{\varepsilon^0_x, \varepsilon^0_y, \gamma^0_{xy}\}^t, \quad k^b = \{k^b_x, k^b_y, k^b_{xy}\}^t, \quad k^s = \{k^s_x, k^s_y, k^s_{xy}\}^t \tag{13d}$$

$$A = \begin{bmatrix} A_{11} & A_{12} & 0 \\ A_{12} & A_{22} & 0 \\ 0 & 0 & A_{66} \end{bmatrix}, \quad B = \begin{bmatrix} B_{11} & B_{12} & 0 \\ B_{12} & B_{22} & 0 \\ 0 & 0 & B_{66} \end{bmatrix}, \quad D = \begin{bmatrix} D_{11} & D_{12} & 0 \\ D_{12} & D_{22} & 0 \\ 0 & 0 & D_{66} \end{bmatrix} \tag{13e}$$

$$B^s = \begin{bmatrix} B^s_{11} & B^s_{12} & 0 \\ B^s_{12} & B^s_{22} & 0 \\ 0 & 0 & B_{66} \end{bmatrix}, \quad D^s = \begin{bmatrix} D^s_{11} & D^s_{12} & 0 \\ D^s_{12} & D^s_{22} & 0 \\ 0 & 0 & D_{66} \end{bmatrix}, \quad H^s = \begin{bmatrix} H^s_{11} & H^s_{12} & 0 \\ H^s_{12} & H^s_{22} & 0 \\ 0 & 0 & H_{66} \end{bmatrix} \tag{13f}$$

Where $A_{ij}$ , $B_{ij}$ , $D_{ij}$ etc., are the plate stiffness, defined by

$$\begin{Bmatrix} A_{11} & B_{11} & D_{11} & B^s_{11} & D^s_{11} & H^s_{11} \\ A_{12} & B_{12} & D_{12} & B^s_{12} & D^s_{12} & H^s_{12} \\ A_{66} & B_{66} & D_{66} & B^s_{66} & D^s_{66} & H^s_{66} \end{Bmatrix} = \int_{-h/2}^{+h/2} Q_{11}(1, z, z^2, f(z), zf(z), f^2(z)) \begin{Bmatrix} 1 \\ \nu \\ \dfrac{1-\nu}{2} \end{Bmatrix} dz \tag{14a}$$

$$(A_{22}, B_{22}, D_{22}, B^s_{22}, D^s_{22}, H^s_{22}) = (A_{11}, B_{11}, D_{11}, B^s_{11}, D^s_{11}, H^s_{11}) \tag{14b}$$

$$A^s_{44} = A^s_{55} = \int_{-h/2}^{h/2} \frac{E(z)}{2(1+\nu)} [g(z)]^2 \, dz \tag{14c}$$

The stress and moment resultants,

$$N^T_x = N^T_y, \quad M^{bT}_x = M^{bT}_y, \quad M^{sT}_x = M^{sT}_y, \quad N^C_x = N^C_y, \quad M^{bC}_x = M^{bC}_y, \quad M^{sC}_x = M^{sC}_y$$

due to thermal and hygroscopic loading are defined respectively by

$$\begin{Bmatrix} N_x^T \\ M_x^{bT} \\ M_x^{sT} \end{Bmatrix} = \int_{-\frac{h}{2}}^{\frac{h}{2}} \frac{E(z)}{1-\nu}\alpha(z)T \begin{Bmatrix} 1 \\ z \\ f(z) \end{Bmatrix} dz \,, \qquad \begin{Bmatrix} N_x^C \\ M_x^{bC} \\ M_x^{sC} \end{Bmatrix} = \int_{-\frac{h}{2}}^{\frac{h}{2}} \frac{E(z)}{1-\nu}\beta(z)C \begin{Bmatrix} 1 \\ z \\ f(z) \end{Bmatrix} dz \tag{15}$$

The governing equations of equilibrium can be derived from Eq. (10) by integrating the displacement gradients by parts and setting the coefficients $\delta u_0$, $\delta v_0$, $\delta w_b$ and $\delta w_s$ zero separately. Thus one can obtain the equilibrium equations associated with the present shear deformation theory,

$$\begin{aligned}
\delta u_0 &: \ \frac{\partial N_x}{\partial x} + \frac{\partial N_{xy}}{\partial y} = 0 \\
\delta v_0 &: \ \frac{\partial N_{xy}}{\partial x} + \frac{\partial N_y}{\partial y} = 0 \\
\delta w_b &: \ \frac{\partial^2 M_x^b}{\partial x^2} + 2\frac{\partial^2 M_{xy}^b}{\partial x \partial y} + \frac{\partial^2 M_y^b}{\partial y^2} - f_e + q = 0 \\
\delta w_s &: \ \frac{\partial^2 M_x^s}{\partial x^2} + 2\frac{\partial^2 M_{xy}^s}{\partial x \partial y} + \frac{\partial^2 M_y^s}{\partial y^2} + \frac{\partial S_{xz}^s}{\partial x} + \frac{\partial S_{yz}^s}{\partial y} - f_e + q = 0
\end{aligned} \tag{16}$$

Substituting from Eq. (12) into Eq. (16), we obtain the following equation,

$$\begin{aligned}
&A_{11}d_{11}u_0 + A_{66}d_{22}u_0 + (A_{12} + A_{66})d_{12}v_0 - B_{11}d_{111}w_b - (B_{12} + 2B_{66})d_{122}w_b \\
&- (B_{12}^s + 2B_{66}^s)d_{122}w_s - B_{11}^s d_{111}w_s = p_1
\end{aligned} \tag{17a}$$

$$\begin{aligned}
&A_{22}d_{22}v_0 + A_{66}d_{11}v_0 + (A_{12} + A_{66})d_{12}u_0 - B_{22}d_{222}w_b - (B_{12} + 2B_{66})d_{112}w_b \\
&- (B_{12}^s + 2B_{66}^s)d_{112}w_s - B_{22}^s d_{222}w_s = p_2
\end{aligned} \tag{17b}$$

$$\begin{aligned}
&B_{11}d_{111}u_0 + (B_{12} + 2B_{66})d_{122}u_0 + (B_{12} + 2B_{66})d_{112}v_0 + B_{22}d_{222}v_0 - D_{11}d_{1111}w_b \\
&- 2(D_{12} + 2D_{66})d_{1122}w_b - D_{22}d_{2222}w_b - D_{11}^s d_{1111}w_s - 2(D_{12}^s + 2D_{66}^s)d_{1122}w_s \\
&- D_{22}^s d_{2222}w_s = p_3
\end{aligned} \tag{17c}$$

$$\begin{aligned}
&B_{11}^s d_{111}u_0 + (B_{12}^s + 2B_{66}^s)d_{122}u_0 + (B_{12}^s + 2B_{66}^s)d_{112}v_0 + B_{22}^s d_{222}v_0 - D_{11}^s d_{1111}w_b \\
&- 2(D_{12}^s + 2D_{66}^s)d_{1122}w_b - D_{22}^s d_{2222}w_b - H_{11}^s d_{1111}w_s - 2(H_{12}^s + 2H_{66}^s)d_{1122}w_s \\
&- H_{22}^s d_{2222}w_s + A_{55}^s d_{11}w_s + A_{44}^s d_{22}w_s = p_4
\end{aligned} \tag{17d}$$

Where $\{p\}=\{p_1, p_2, p_3, p_4\}^t$ is a generalized force vector, $d_{ij}$, $d_{ijl}$ and $d_{ijlm}$ are the following differential operators

$$d_{ij} = \frac{\partial^2}{\partial x_i \partial x_j}, \quad d_{ijl} = \frac{\partial^3}{\partial x_i \partial x_j \partial x_l}, \quad d_{ijlm} = \frac{\partial^4}{\partial x_i \partial x_j \partial x_l \partial x_m}, \quad d_i = \frac{\partial}{\partial x_i} \qquad (i,j,l,m = 1,2) \tag{18a}$$

The components of the generalized force vector $\{p\}$ are given by

$$p_1 = \frac{\partial N_x^T}{\partial x} + \frac{\partial N_x^C}{\partial x}, \qquad p_3 = f_e + q - \frac{\partial^2 (M_x^{bT} + M_x^{bC})}{\partial x^2} - \frac{\partial^2 (M_y^{bT} + M_y^{bC})}{\partial y^2}$$
$$p_2 = \frac{\partial N_y^T}{\partial y} + \frac{\partial N_y^C}{\partial y}; \qquad p_4 = f_e + q - \frac{\partial^2 (M_x^{sT} + M_x^{sC})}{\partial x^2} - \frac{\partial^2 (M_y^{sT} + M_y^{sC})}{\partial y^2} \tag{18b}$$

## 3. Exact solutions

Following Navier procedure, the uniform external force as well as the transverse uniform temperature and moisture concentration loads are presented in the form of a double trigonometric series. We are here concerned with the exact solution of Eqs. (17) for a simply supported FGM plate. To solve this problem, Navier assumed that the transverse mechanical, temperature and moisture loads, $q$, $T_i$ and $C_i$ in the form of a in the double Fourier series as

$$\begin{Bmatrix} q \\ T_i \\ C_i \end{Bmatrix} = \begin{Bmatrix} q_0 \\ t_i \\ c_i \end{Bmatrix} \sin(\lambda x) \sin(\mu y) \qquad (i = 1,2,3) \tag{19}$$

Where $\lambda = \pi / a$, $\mu = \pi / b$, $q_0$, $t_i$ and $c_i$ are constants and $T_i$ and $C_i$ are defined in Eq. (7). Following the Navier procedure, we assume the following solution form for $u_0$, $v_0$, $w_b$ and $w_s$ that satisfies the boundary conditions,

$$\begin{Bmatrix} u_0 \\ v_0 \\ w_b \\ w_s \end{Bmatrix} = \begin{Bmatrix} U \cos(\lambda x) \sin(\mu y) \\ V \sin(\lambda x) \cos(\mu y) \\ W_b \sin(\lambda x) \sin(\mu y) \\ W_s \sin(\lambda x) \sin(\mu y) \end{Bmatrix} \tag{20}$$

Where $U$, $V$, $W_b$ and $W_s$ are arbitrary parameters to be determined subjected to the condition that the solution in Eq. (20) satisfies governing equation (17). One obtains the following operator equation,

$$[K]\{\Delta\} = \{P\} \tag{21}$$

Where $\{\Delta\} = \{U, V, W_b, W_s\}^t$ and [K] is the symmetric matrix given by

$$[K] = \begin{bmatrix} k_{11} & k_{12} & k_{13} & k_{14} \\ k_{12} & k_{22} & k_{23} & k_{24} \\ k_{13} & k_{23} & k_{33} & k_{34} \\ k_{14} & k_{24} & k_{34} & k_{44} \end{bmatrix} \tag{22}$$

In which

$$k_{11}=-(A_{11}\lambda^2+A_{66}\mu^2),\quad k_{22}=-(A_{66}\lambda^2+A_{22}\mu^2),\quad k_{33}=-(D_{11}\lambda^4+2(D_{12}+2D_{66})\lambda^2\mu^2+D_{22}\mu^4+K_w+J_1\lambda^2+J_2\mu^2);$$

$$k_{12}=-\lambda\,\mu\,(A_{12}+A_{66}),\ k_{13}=\lambda\,[B_{11}\lambda^2+(B_{12}+2B_{66})\,\mu^2],\quad k_{14}=\lambda\,[B^s_{11}\lambda^2+(B^s_{12}+2B^s_{66})\,\mu^2];$$

$$k_{23}=\mu\,[(B_{12}+2B_{66})\,\lambda^2+B_{22}\,\mu^2],\quad k_{24}=\mu\,[(B^s_{12}+2B^s_{66})\,\lambda^2+B^s_{22}\,\mu^2]; \tag{23}$$

$$k_{34}=-(D^s_{11}\lambda^4+2(D^s_{12}+2D^s_{66})\lambda^2\,\mu^2+D^s_{22}\,\mu^4+K_w+J_1\lambda^2+J_2\mu^2)$$

$$k_{44}=-(H^s_{11}\lambda^4+2(H^s_{12}+2H^s_{66})\lambda^2\mu^2+H^s_{22}\mu^4+A^s_{55}\lambda^2+A^s_{44}\mu^2+D^s_{22}\,\mu^4+K_w+J_1\lambda^2+J_2\mu^2)$$

The components of the generalized force vector $\{P\}=\{P_1,P_2,P_3,P_4\}^t$ are given by

$$\begin{aligned}
P_1&=\lambda\left[(A^T t_1+B^T t_2+{}^aB^T t_3)+(A^C c_1+B^C c_2+{}^aB^C c_3)\right]\\
P_2&=\mu\left[(A^T t_1+B^T t_2+{}^aB^T t_3)+(A^C c_1+B^C c_2+{}^aB^C c_3)\right]\\
P_3&=-q_0-h(\lambda^2+\mu^2)\left[(B^T t_1+D^T t_2+{}^aD^T t_3)+(B^C c_1+D^C c_2+{}^aD^C c_3)\right]\\
P_4&=-q_0-h(\lambda^2+\mu^2)\left[({}^sB^T t_1+{}^sD^T t_2+{}^sF^T t_3)+({}^sB^C c_1+{}^sD^C c_2+{}^sF^C c_3)\right]
\end{aligned} \tag{24}$$

Where

$$\left\{A^T,B^T,D^T\right\}=\int_{-h/2}^{h/2}\frac{E(z)}{1-\nu}\alpha(z)\left\{1,\bar z,\bar z^2\right\}dz \tag{25a}$$

$$\left\{A^C,B^C,D^C\right\}=\int_{-h/2}^{h/2}\frac{E(z)}{1-\nu}\beta(z)\left\{1,\bar z,\bar z^2\right\}dz \tag{25b}$$

$$\left\{{}^aB^T,{}^aD^T\right\}=\int_{-h/2}^{h/2}\frac{E(z)}{1-\nu}\alpha(z)\overline{\psi}(z)\left\{1,\bar z\right\}dz \tag{25c}$$

$$\left\{{}^aB^C,{}^aD^C\right\}=\int_{-h/2}^{h/2}\frac{E(z)}{1-\nu}\beta(z)\overline{\psi}(z)\left\{1,\bar z\right\}dz \tag{25d}$$

$$\left\{{}^sB^T,{}^sD^T,{}^sF^T\right\}=\int_{-h/2}^{h/2}\frac{E(z)}{1-\nu}\alpha(z)\,\bar f(z)\left\{1,\bar z,\overline{\psi}(z)\right\}dz \tag{25e}$$

$$\left\{{}^sB^C,{}^sD^C,{}^sF^C\right\}=\int_{-h/2}^{h/2}\frac{E(z)}{1-\nu}\beta(z)\,\bar f(z)\left\{1,\bar z,\overline{\psi}(z)\right\}dz \tag{25f}$$

In which

$$\bar z=z/h,\qquad \bar f(z)=f(z)/h,\quad \overline{\psi}(z)=\frac{1}{\pi}\sin\left(\frac{\pi z}{h}\right)$$

Table 1 Effect of the volume fraction exponent and elastic foundation parameters on the dimensionless deflection and stresses of an FGM rectangular plate with and without porosities ($a = 10h$, $b = 3a$, $q_0 = 100$, $T = C = 0$).

| $p$ | $K_0$ | $J_0$ | Theory | $\zeta$ | $\overline{w}$ | $\overline{\sigma}_x$ | $\overline{\tau}_{xy}$ | $\overline{\tau}_{xz}$ |
|---|---|---|---|---|---|---|---|---|
| 0 | 0 | 0 | Present Model | $\zeta = 0$ | 0.85885 | 0.51364 | 0.72787 | -0.44328 |
| | | | Reddy model | $\zeta = 0$ | 0.85891 | 0.51545 | 0.72797 | -0.42956 |
| | | | FSDT model | $\zeta = 0$ | 0.85892 | 0.51065 | 0.72949 | -0.34377 |
| | 100 | 0 | Present Model | $\zeta = 0$ | 0.46203 | 0.27632 | 0.39157 | -0.23847 |
| | | | Reddy model | $\zeta = 0$ | 0.46206 | 0.27620 | 0.39162 | -0.23109 |
| | | | FSDT model | $\zeta = 0$ | 0.46206 | 0.27471 | 0.39246 | -0.18493 |
| | 0 | 100 | Present Model | $\zeta = 0$ | 0.08964 | 0.05361 | 0.07597 | -0.04627 |
| | | | Reddy model | $\zeta = 0$ | 0.08965 | 0.05358 | 0.07599 | -0.04485 |
| | | | FSDT model | $\zeta = 0$ | 0.08965 | 0.05330 | 0.07616 | -0.03588 |
| | 100 | 100 | Present Model | $\zeta = 0$ | 0.08227 | 0.04920 | 0.06972 | -0.04246 |
| | | | Reddy model | $\zeta = 0$ | 0.08228 | 0.04919 | 0.06972 | -0.04116 |
| | | | FSDT model | $\zeta = 0$ | 0.08228 | 0.04890 | 0.06986 | -0.03293 |
| 0.5 | 100 | 100 | Present Model | $\zeta = 0$ | 0.08364 | 0.04671 | 0.05812 | -0.03609 |
| | | | | $\zeta = 0.1$ | 0.08430 | 0.04308 | 0.05290 | -0.03291 |
| | | | | $\zeta = 0.2$ | 0.08496 | 0.03938 | 0.04758 | -0.02968 |
| | | | Reddy model | $\zeta = 0$ | 0.08366 | 0.04671 | 0.05812 | -0.03498 |
| | | | FSDT model | $\zeta = 0$ | 0.08366 | 0.04643 | 0.05824 | -0.02828 |
| 2 | 100 | 100 | Present Model | $\zeta = 0$ | 0.08456 | 0.04541 | 0.04769 | -0.03049 |
| | | | | $\zeta = 0.1$ | 0.08523 | 0.04162 | 0.04222 | -0.02715 |
| | | | | $\zeta = 0.2$ | 0.08590 | 0.03768 | 0.03661 | -0.02378 |
| | | | Reddy model | $\zeta = 0$ | 0.08457 | 0.04539 | 0.04770 | -0.02951 |
| | | | FSDT model | $\zeta = 0$ | 0.08457 | 0.04515 | 0.04781 | -0.02303 |
| Metal | 100 | 100 | Present Model | $\zeta = 0$ | 0.08584 | 0.02905 | 0.04116 | -0.02507 |
| | | | | $\zeta = 0.1$ | 0.08651 | 0.02522 | 0.03574 | -0.02177 |
| | | | | $\zeta = 0.2$ | 0.08720 | 0.02134 | 0.03024 | -0.01842 |
| | | | Reddy model | $\zeta = 0$ | 0.08584 | 0.02905 | 0.04115 | -0.02428 |
| | | | FSDT model | $\zeta = 0$ | 0.08584 | 0.02888 | 0.04126 | -0.01943 |

## 4. Numerical results

To illustrate the proposed approach, the Titanium/Zerconia of perfect and imperfect FG plate is considered. Young's modulus, Poisson's ratio, coefficient of thermal expansion, and moisture concentration expansion for

Titanium, *Ti-6Al-4V*: $E_m = 66.2GPa$ ; $\nu = 1/3$ ; ; $\beta_m = 0.33$

Zirconia, $ZrO_2$: $E_c = 117.0GPa$ ; $\nu = 1/3$ ; $\alpha_c = 7.11 \times (10^{-6}/°C)$ ; $\beta_c = 0$

Table 2 Effect of the volume fraction exponent and elastic foundation parameters on the dimensionless deflection and stresses of an FGM rectangular plate *($a = 10h$, $b = 3a$, $q_0=100$; $t_1=t_3=0$, $t_2=10$, $c_1=c_3=0$, $c_2=100$).*

| $p$ | $K_0$ | $J_0$ | Theory | $\zeta$ | $\bar{w}$ | $\bar{\sigma}_x$ | $\bar{\tau}_{xy}$ | $\bar{\tau}_{xz}$ |
|---|---|---|---|---|---|---|---|---|
| Ceramic | 0 | 0 | Present Model | $\zeta = 0$ | 1.80707 | 0.47204 | 1.55974 | -0.44328 |
| | | | Reddy model | $\zeta = 0$ | 1.80712 | 0.47187 | 1.55982 | -0.42955 |
| | | | FSDT model | $\zeta = 0$ | 1.80713 | 0.46900 | 1.56139 | -0.34377 |
| | 100 | 0 | Present Model | $\zeta = 0$ | 0.97214 | -0.02729 | 0.85215 | -0.01235 |
| | | | Reddy model | $\zeta = 0$ | 0.97216 | -0.02740 | 0.85211 | -0.01197 |
| | | | FSDT model | $\zeta = 0$ | 0.97216 | -0.02750 | 0.85216 | -0.00957 |
| | 0 | 100 | Present Model | $\zeta = 0$ | 0.18861 | -0.49588 | 0.18810 | 0.39206 |
| | | | Reddy model | $\zeta = 0$ | 0.18861 | -0.49570 | 0.18806 | 0.37990 |
| | | | FSDT model | $\zeta = 0$ | 0.18860 | -0.49322 | 0.18667 | 0.30404 |
| | 100 | 100 | Present Model | $\zeta = 0$ | 0.17309 | -0.50516 | 0.17495 | 0.40007 |
| | | | Reddy model | $\zeta = 0$ | 0.17309 | -0.50498 | 0.17490 | 0.38766 |
| | | | FSDT model | $\zeta = 0$ | 0.17309 | -0.50245 | 0.17351 | 0.31024 |
| 0.5 | 100 | 100 | Present Model | $\zeta = 0$ | 0.18411 | -0.51999 | 0.18301 | 0.45727 |
| | | | | $\zeta = 0.1$ | 0.16549 | -0.42187 | 0.15147 | 0.36625 |
| | | | | $\zeta = 0.2$ | 0.14872 | -0.33279 | 0.12405 | 0.28426 |
| | | | Reddy model | $\zeta = 0$ | 0.18410 | -0.51975 | 0.18299 | 0.44334 |
| | | | FSDT model | $\zeta = 0$ | 0.18408 | -0.51623 | 0.18190 | 0.35898 |
| 1 | 100 | 100 | Present Model | $\zeta = 0$ | 0.18504 | -0.51475 | 0.15636 | 0.45986 |
| | | | | $\zeta = 0.1$ | 0.16621 | -0.41652 | 0.12578 | 0.36814 |
| | | | | $\zeta = 0.2$ | 0.14925 | -0.32731 | 0.09924 | 0.28549 |
| | | | Reddy model | $\zeta = 0$ | 0.18504 | -0.51450 | 0.15631 | 0.44545 |
| | | | FSDT model | $\zeta = 0$ | 0.18505 | -0.51084 | 0.15494 | 0.35542 |
| 2 | 100 | 100 | Present Model | $\zeta = 0$ | 0.18559 | -0.50363 | 0.13461 | 0.45337 |
| | | | | $\zeta = 0.1$ | 0.16659 | -0.40543 | 0.10501 | 0.36169 |
| | | | | $\zeta = 0.2$ | 0.14945 | -0.31618 | 0.79451 | 0.27908 |
| | | | Reddy model | $\zeta = 0$ | 0.18560 | -0.50336 | 0.13451 | 0.43831 |
| | | | FSDT model | $\zeta = 0$ | 0.18567 | -0.49980 | 0.13244 | 0.33958 |
| Metal | 100 | 100 | Present Model | $\zeta = 0$ | 0.18840 | -0.43117 | 0.12092 | 0.47465 |
| | | | Reddy model | $\zeta = 0$ | 0.18840 | -0.43095 | 0.12087 | 0.45993 |
| | | | FSDT model | $\zeta = 0$ | 0.18840 | -0.42794 | 0.11921 | 0.36808 |

In this section, numerical examples are presented and discussed for verifying the accuracy of the present theory in predicting the hygro-thermo-mechanical bending responses of perfect and imperfect FGM plates. Comparisons are made with various plate theories available in the scientific literature. The reference temperature and moisture concentration are taken by $T_0=25°C$ (room temperature) and $C_0=0\%$, numerical results are presented in terms of non-dimensional stresses and

Table 3 Effect of the volume fraction exponent and elastic foundation parameters on the dimensionless deflection and stresses of an FGM rectangular plate with and without porosities *($a=10h$, $b=3a$, $q_0=100$, $t_1=0$, $t_2=t_3=10$ , $c_1=0$ , $c_2=c_3=100$).*

| $p$ | $K_0$ | $J_0$ | Theory | $\zeta$ | $\overline{w}$ | $\overline{\sigma}_x$ | $\overline{\tau}_{xy}$ | $\overline{\tau}_{xz}$ |
|---|---|---|---|---|---|---|---|---|
| Ceramic | 0 | 0 | Present Model | $\zeta = 0$ | 2.54067 | 0.52554 | 2.20366 | -0.43753 |
| | | | Reddy model | $\zeta = 0$ | 2.54076 | 0.52522 | 2.20374 | -0.42454 |
| | 100 | 0 | Present Model | $\zeta = 0$ | 1.36680 | -0.17649 | 1.20881 | 0.16834 |
| | | | Reddy model | $\zeta = 0$ | 1.36682 | -0.17643 | 1.20877 | 0.16257 |
| | 0 | 100 | Present Model | $\zeta = 0$ | 0.26517 | -0.83532 | 0.27518 | 0.73692 |
| | | | Reddy model | $\zeta = 0$ | 0.26518 | -0.83500 | 0.27507 | 0.71354 |
| | 100 | 100 | Present Model | $\zeta = 0$ | 0.24336 | -0.84837 | 0.25669 | 0.74817 |
| | | | Reddy model | $\zeta = 0$ | 0.24336 | -0.84804 | 0.25658 | 0.72442 |
| 0.5 | 100 | 100 | Present Model | $\zeta = 0$ | 0.26196 | -0.87282 | 0.28041 | 0.84587 |
| | | | | $\zeta = 0.1$ | 0.22844 | -0.71238 | 0.22844 | 0.68075 |
| | | | | $\zeta = 0.2$ | 0.19820 | -0.56627 | 0.18386 | 0.53174 |
| | | | Reddy model | $\zeta = 0$ | 0.26195 | -0.87239 | 0.28034 | 0.81947 |
| 1 | 100 | 100 | Present Model | $\zeta = 0$ | 0.26330 | -0.86250 | 0.23772 | 0.84866 |
| | | | | $\zeta = 0.1$ | 0.22940 | -0.70179 | 0.18756 | 0.68224 |
| | | | | $\zeta = 0.2$ | 0.19878 | -0.55537 | 0.14466 | 0.53196 |
| | | | Reddy model | $\zeta = 0$ | 0.26330 | -0.86205 | 0.23762 | 0.82148 |
| 2 | 100 | 100 | Present Model | $\zeta = 0$ | 0.26394 | -0.84183 | 0.20154 | 0.83481 |
| | | | | $\zeta = 0.1$ | 0.22972 | -0.68110 | 0.15319 | 0.66835 |
| | | | | $\zeta = 0.2$ | 0.19878 | -0.53449 | 0.11213 | 0.51806 |
| | | | Reddy model | $\zeta = 0$ | 0.26396 | -0.84138 | 0.20133 | 0.80652 |
| 5 | 100 | 100 | Present Model | $\zeta = 0$ | 0.26599 | -0.81790 | 0.18486 | 0.83228 |
| | | | | $\zeta = 0.1$ | 0.23148 | -0.65816 | 0.13785 | 0.66489 |
| | | | | $\zeta = 0.2$ | 0.20025 | -0.51226 | 0.09805 | 0.51369 |
| | | | Reddy model | $\zeta = 0$ | 0.26601 | -0.81745 | 0.18459 | 0.80297 |
| Metal | 100 | 100 | Present Model | $\zeta = 0$ | 0.26775 | -0.71694 | 0.18299 | 0.86749 |
| | | | Reddy model | $\zeta = 0$ | 0.26774 | -0.71656 | 0.18286 | 0.84003 |

deflection. The various non-dimensional parameters used are

$$\overline{w} = \frac{10^2 D}{a^4 q_0} w\left(\frac{a}{2}, \frac{b}{2}\right); \qquad \overline{\sigma}_x = \frac{1}{10^2 q_0}\sigma_x\left(\frac{a}{2}, \frac{b}{2}, \frac{h}{2}\right); \qquad \overline{\tau}_{xy} = \frac{1}{10\, q_0}\tau_{xy}\left(0,0,\frac{-h}{3}\right)$$

$$\overline{\tau}_{xz} = -\frac{1}{10\, q_0}\tau_{xz}\left(0,\frac{b}{2},0\right); \qquad K_0 = \frac{a^4 K_w}{D}, \qquad J_O = \frac{a^2 J_1}{D} = \frac{b^2 J_2}{D}, \qquad D = \frac{h^3 E_c}{12(1-\nu^2)}$$

Numerical results are presented in tabulated in Tables 1-4 and graphically plotted in Figs. 2-10 using the present model . It is assumed, unless otherwise stated, that $q_0=100\ GPa$, $a/h = 10$ , $b/a = 3$, $p = 2$, $t_1 = t_2 = 0$, $c_1 = c_2 = 0$.

The correlation between the present model and the higher-order theory Reddy model (2000) and first-order shear deformation theories FSDT is illustrated in Tables 1-3. These tables give also the effects of the volume fraction exponent ratio $P$ and elastic foundation parameters on the dimensionless deflection and stresses of perfect and imperfect FGM rectangular plate. Table 1

Table 4 Effects of side-to-thickness ratio and elastic foundation parameters on the dimensionless deflection of an FGM square plate *(b = a,* $q_0 = 100$ , $t_1 = 0$ , $t_2 = t_3 = 10$ , $c_1 = 0$ , $c_2 = c_3 = 100$ *,).*

| P | $K_0$ | $J_0$ | $\zeta$ | a/h | | | | |
|---|---|---|---|---|---|---|---|---|
| | | | | 5 | 10 | 20 | 50 | 100 |
| 0.5 | 0 | 0 | $\zeta = 0$ | 5.29023 | 1.55628 | 0.62189 | 0.36020 | 032281 |
| | | | $\zeta = 0.1$ | 4.77653 | 1.45251 | 0.62069 | 0.38772 | 0.35444 |
| | | | $\zeta = 0.2$ | 4.26990 | 1.35652 | 0.62744 | 0.42324 | 0.39407 |
| | 100 | 0 | $\zeta = 0$ | 3.83159 | 1.17192 | 0.47301 | 0.27474 | 0.24632 |
| | | | $\zeta = 0.1$ | 3.36205 | 1.06588 | 0.46039 | 0.28846 | 0.26381 |
| | | | $\zeta = 0.2$ | 2.90407 | 0.96489 | 0.45148 | 0.30554 | 28462 |
| | 0 | 100 | $\zeta = 0$ | 0.62132 | 0.20823 | 0.08622 | 0.05045 | 0.04529 |
| | | | $\zeta = 0.1$ | 0.51335 | 0.17800 | 0.07884 | 0.04975 | 0.04555 |
| | | | $\zeta = 0.2$ | 0.41521 | 0.15053 | 0.07218 | 0.04919 | 0.04587 |
| | 100 | 100 | $\zeta = 0$ | 0.59473 | 0.19948 | 0.08261 | 0.04834 | 0.04339 |
| | | | $\zeta = 0.1$ | 0.49114 | 0.17043 | 0.07550 | 0.04765 | 0.04362 |
| | | | $\zeta = 0.2$ | 0.39705 | 0.14404 | 0.06908 | 0.04709 | 0.04391 |
| 2 | 0 | 0 | $\zeta = 0$ | 6.07957 | 1.79155 | 0.71642 | 0.41516 | 0.37211 |
| | | | $\zeta = 0.1$ | 5.57581 | 1.69972 | 0.72762 | 0.45521 | 0.41629 |
| | | | $\zeta = 0.2$ | 5.08437 | 1.62145 | 0.75267 | 0.50920 | 0.47441 |
| | 100 | 0 | $\zeta = 0$ | 4.20771 | 1.29862 | 0.52553 | 0.30557 | 0.27402 |
| | | | $\zeta = 0.1$ | 3.71360 | 1.19036 | 0.51624 | 0.32416 | 0.29660 |
| | | | $\zeta = 0.2$ | 3.22777 | 1.08752 | 0.51207 | 0.34783 | 0.32425 |
| | 0 | 100 | $\zeta = 0$ | 0.62155 | 0.21095 | 0.08769 | 0.05139 | 0.04613 |
| | | | $\zeta = 0.1$ | 0.51162 | 0.17993 | 0.08011 | 0.05069 | 0.04643 |
| | | | $\zeta = 0.2$ | 0.41156 | 0.15166 | 0.07326 | 0.05013 | 0.04678 |
| | 100 | 100 | $\zeta = 0$ | 0.59451 | 0.20193 | 0.08396 | 0.04920 | 0.04417 |
| | | | $\zeta = 0.1$ | 0.48911 | 0.17213 | 0.07666 | 0.04851 | 0.04443 |
| | | | $\zeta = 0.2$ | 0.39325 | 0.14500 | 0.07005 | 0.04794 | 0.04474 |
| 10 | 0 | 0 | $\zeta = 0$ | 6.81971 | 2.00812 | 0.80056 | 0.46210 | 0.41374 |
| | | | $\zeta = 0.1$ | 6.32870 | 1.92700 | 0.82192 | 0.51216 | 0.46790 |
| | | | $\zeta = 0.2$ | 5.85622 | 1.86429 | 0.86163 | 0.58054 | 0.54038 |
| | 100 | 0 | $\zeta = 0$ | 4.54370 | 1.41069 | 0.57016 | 0.33039 | 0.29598 |
| | | | $\zeta = 0.1$ | 4.02487 | 1.29937 | 0.56272 | 0.35216 | 0.32192 |
| | | | $\zeta = 0.2$ | 3.51079 | 1.19327 | 0.56102 | 0.37984 | 0.35380 |
| | 0 | 100 | $\zeta = 0$ | 0.62637 | 0.21455 | 0.89184 | 0.52102 | 0.04673 |
| | | | $\zeta = 0.1$ | 0.51458 | 0.18292 | 0.81441 | 0.51379 | 0.04702 |
| | | | $\zeta = 0.2$ | 0.41279 | 0.15407 | 0.74427 | 0.50790 | 0.04736 |
| | 100 | 100 | $\zeta = 0$ | 0.59882 | 0.20526 | 0.08534 | 0.04986 | 0.04472 |
| | | | $\zeta = 0.1$ | 0.49170 | 0.17490 | 0.07789 | 0.04914 | 0.04497 |
| | | | $\zeta = 0.2$ | 0.39422 | 0.14723 | 0.07113 | 0.04855 | 0.04527 |

gives the effects of the volume fraction exponent ratio $P$ and elastic foundation parameters on the dimensionless displacements and stresses of perfect and imperfect FGM plate subjected to a mechanical load. It can be shown that the deflection and stresses are decreasing with the existence of the elastic foundations. The inclusion of the Winkler foundation parameter yields higher magnitude results than those with the inclusion of Pasternak foundation parameters. As the volume fraction exponent increases for perfect and imperfect FGM plates, the deflection will increase. The stresses are also sensitive to the variation of $p$. A table 2 and 3 presents similar results as those given in Table 1 including the effect of the temperature and moisture fields. The obtained results are compared with those predicted by FSDT, Reddy (2000). An excellent agreement is obtained between the present theory and Reddy theory for all values of power law index $p$ and with or without the presence of the elastic foundation. It is important to observe that the stresses for a fully ceramic plate are not the same as that for a fully metal plate with elastic foundations. This is

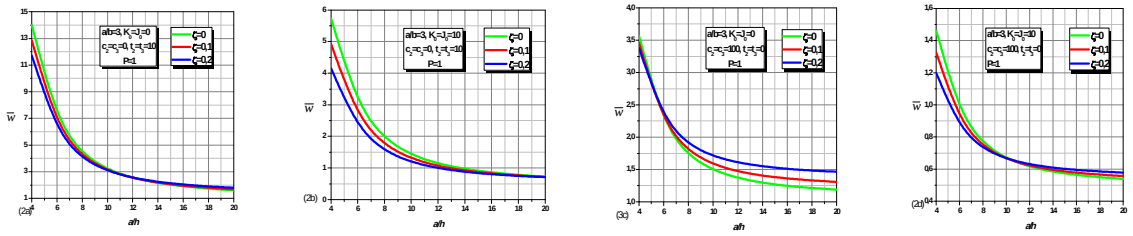

Fig. 2 Dimensionless center deflection $\overline{w}$ versus side-to-thickness ratio a/h for imperfect and perfect FGM rectangular plates on elastic foundations

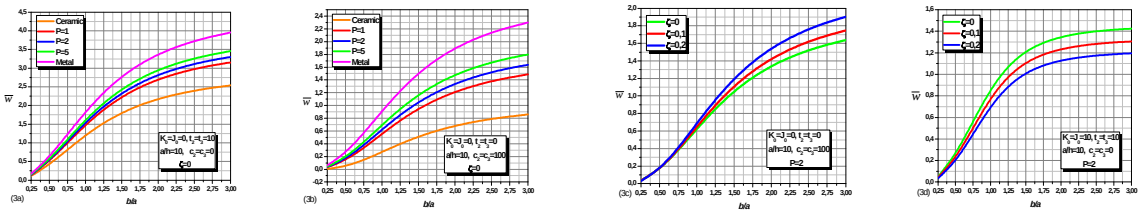

Fig. 3 Dimensionless center deflection $\overline{w}$ versus plate aspect ratio b/a for imperfect and perfect FGM plates on elastic foundations

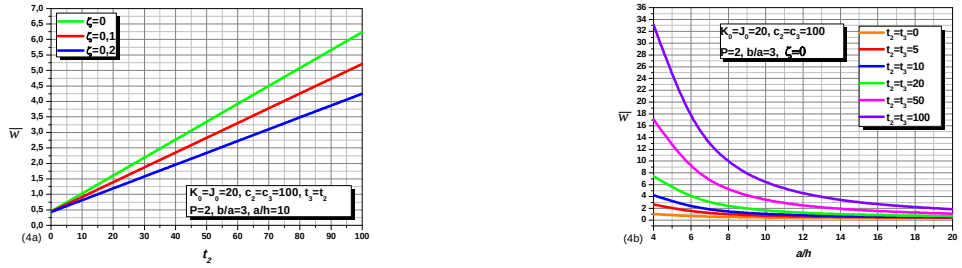

Fig. 4 Dimensionless center deflection $\overline{w}$ of imperfect and perfect FGM plates on elastic foundations versus side-to-thickness ratio a/h for different values of temperatures


Fig. 5 Dimensionless center deflection $\overline{w}$ of imperfect and perfect FGM plates on elastic foundations versus side-to-thickness ratio a/h for different values of moistures


Fig. 6 Effect of elastic modulus of Winkler foundation $K_0$ on dimensionless center deflection $\overline{w}$ of imperfect and perfect FGM plates

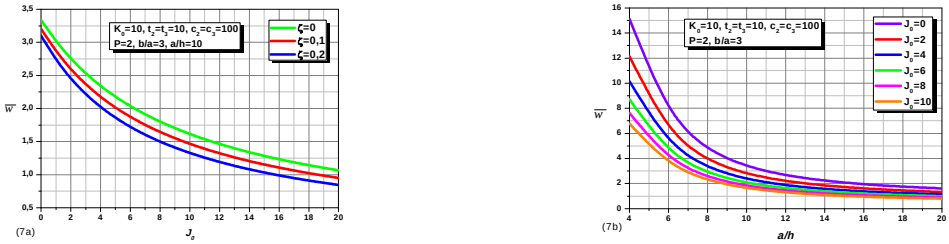


Fig. 7 Effect of Pasternak shear modulus parameter $J_0$ on dimensionless center deflection $\overline{w}$ of FGM plates


Fig. 8 Dimensionless axial stress $\overline{\sigma}_x$ through-the-thickness of imperfect and perfect FGM plates on elastic foundations for different values of moistures and temperatures.

because the plate here is affected with the inclusion of the temperature field. This has an important bearing in rocket-launch foundation structures as via judicious selection of the spatial structure of FGM, one can effectively prolong the serviceability life of the structure. In considering the results presented in tables 1 to 3, it should be noted that the quantity of unknown variables in the present formulation is four, whereas the number unknown function in FSDT and Reddy is five. It can be concluded that the present theory is not only accurate but also comparatively simple and quite

elegant in predicting the hygro-thermo-mechanical bending response of perfect and imperfect FGM plates resting on Winkler's or Pasternak's elastic foundations. Table 4 documents the effects of side-to-thickness ratio and elastic foundation parameters on the dimensionless deflection of imperfect FGM square plate under hygro-thermo-mechanical loads using the present model. It can be seen from Table 4 (and also Fig. 2) that the deflection decreases as the side-to-thickness ratio $a/h$ increases and this, is due to the considerable effect of temperature and moisture on the extensional behavior of the plate comparatively the flexural behavior. This observation is also confirmed by Benferhat *et al.*.(2014). In addition, all displacements observed to decrease with the presence of the elastic foundations. The inclusion of the Winkler foundation parameter effectively generates greater magnitudes in solutions compared with solutions yielded from the inclusion of Pasternak foundation parameters.

A Figs. 2 and 3 shows the variation of the center deflection with aspect ratio for different types of imperfect FGM plates. The deflection of the metallic plate is found to be of the largest magnitude and that of the ceramic plate, of the smallest magnitude irrespective of the values of temperature, moisture, and elastic foundation parameters. All the plates with intermediate properties undergo corresponding intermediate values of center deflection. In addition, the deflection is increasing in the absence of the foundations and the effect of moisture parameter may be less than that of the temperature one. Figs. 4 and 5 shows the variation of the center deflection with side-to-thickness ratio for imperfect FG plates subjected to different parameters. The deflection increases as the moisture parameter increases, and the plate is very sensitive to the variation of elastic foundation parameters. In Figs. 6 and 7 show the effect of foundation parameters $k_0$ and $J_0$ on the variation of non-dimensional center deflection $\overline{w}$ of imperfect FGM plate. The results show that the non-dimensional center deflection decreases with the increase of foundation parameters $k_0$ and $J_0$, and the Winkler parameter $k_0$ has more effect on decreasing the

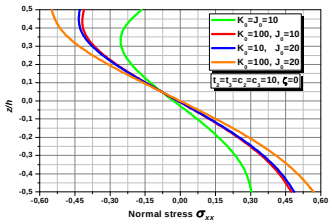


Fig. 9 Dimensionless axial stress $\sigma_x$ through-the-thickness of perfect FGM plate for different values of elastic foundations parameters.

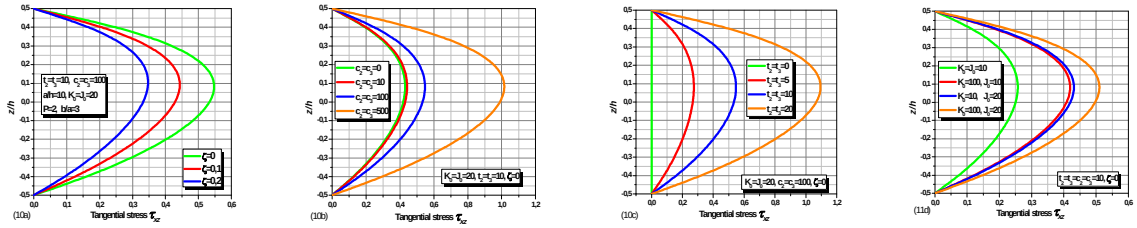


Fig. 10 Dimensionless shear stress $\overline{\tau}_{xz}$ through-the-thickness of FGM plates on elastic foundations

non-dimensional center deflection $\overline{w}$ than the shear Pasternak parameter $J_0$. Decreases of deflections indicate that increasing the foundation stiffness will certainly enhance the deformation rigidity of the plate. It is observed from the results; that effects of $k_0$ and $J_0$ on the non-dimensional center deflection $\overline{w}$ of imperfect FGM plates are more significant for thicker plates. The longitudinal stress $\sigma_x$ and the transverse shear stress $\tau_{xz}$ are plotted in Figs. 8, 9 and 10 through-the-thicknesses of FGM plates. Under the application of the uniform loading and elastic foundations, the longitudinal stress is tensile through the plate thickness and very sensitive to the variation of temperature and moisture parameters.

Figs. 8 and 9 depict the through-the-thickness distributions of the non-dimensional axial stress $\overline{\sigma}_x$ in the imperfect FGM rectangular plates. The effect of moisture and temperature fields on $\overline{\sigma}_x$ is shown in Fig. 8, while the effect of elastic foundations parameters is shown Fig. 9. As exhibited in these figures, the maximum compressive stresses occur at a point on the top surface and the maximum tensile stresses occur, of course, at a point on the bottom surface of the imperfect FGM plates. As illustrated in Fig. 9 the elastic foundation has a significant effect on the maximum values of the non-dimensional axial stress $\overline{\sigma}_x$.

Fig. 10 show that the maximum value occurs at a point above the mid-plane of the imperfect FGM plate and its magnitude increases with the inclusion of the temperature, moisture, and foundation parameters. The non-dimensional transverse shear stress $\overline{\tau}_{xz}$ is plotted through-the-thickness of imperfect FGM plates. It is evident that the maximum value of $\overline{\tau}_{xz}$ arises at a point above the mid-plane of the imperfect FGM plate and its magnitude increases with the inclusion of the foundation parameters.

## 5. Conclusion

In this paper, the hygro-thermo-mechanical bending response of perfect and imperfect FGM plates resting on elastic foundations by using the sinusoidal higher order shear deformation theory to plate is studied. The stress and displacement response of the plates have been analyzed under uniform loading. Dimensionless stresses and deflection are computed for perfect and imperfect FG plates subjected to the hygrothermal effects. Illustrating examples are carried out, with the most important conclusions that the effect of moisture concentration parameter on thermo- mechanical responses of the imperfect FGM plates is considerably different. The influence of moisture concentration as well as other parameter is highly significant. The influence of moisture concentration as well as other parameters is demonstrated to be significant. The bending response of the perfect and imperfect FG plate deteriorates considerably with the increase in temperature and moisture concentration. The results are verified with available results in the literature. It can be concluded that the proposed theory is accurate and simple in solving the hygro-thermo-mechanical bending behavior of perfect and imperfect functionally graded plates.

## Acknowledgments

The authors thank the referees for their valuable comments.

## References

Abdelhak, Z., Hadji, L., Daouadji, T.H. and Bedia, E.A. (2015), "Thermal buckling of functionally graded plates using a n-order four variable refined theory", *Adv. Mater. Res.*, **4**(1), 31-44.

Bahrami, A. and Nosier, A. (2007), "Interlaminar hygrothermal stresses in laminated plates", *Int. J. Solid. Struct.*, **44**(25), 8119-8142.

Belabed, Z., Houari, M.S.A., Tounsi, A., Mahmoud, S.R. and Bég, O.A. (2014), "An efficient and simple higher order shear and normal deformation theory for functionally graded material (FGM) plates", *Compos. Part B: Eng.*, **60**, 274-283.

Bellifa, H., Benrahou, K.H., Hadji, L., Houari, M.S.A. and Tounsi, A. (2016), "Bending and free vibration analysis of functionally graded plates using a simple shear deformation theory and the concept the neutral surface position", *J. Brazilian Society Mech. Sci. Eng.*, **38**(1), 265-275.

Benachour, A., Tahar, H.D., Atmane, H.A., Tounsi, A. and Ahmed, M.S. (2011), "A four variable refined plate theory for free vibrations of functionally graded plates with arbitrary gradient", *Compos. Part B: Eng.*, **42**(6), 1386-1394.

Benferhat, R., Daouadji, T.H. and Mansour, M.S. (2015), "A higher order shear deformation model for bending analysis of functionally graded plates", *Transact. Indian Inst. Metal.*, **68**(1), 7-16.

Benkhedda, A. and Tounsi, A. (2008), "Effect of temperature and humidity on transient hygrothermal stresses during moisture desorption in laminated composite plates", *Compos. Struct.*, **82**(4), 629-635.

Bennoun, M., Houari, M.S.A. and Tounsi, A. (2016), "A novel five-variable refined plate theory for vibration analysis of functionally graded sandwich plates", *Mech. Adv. Mater. Struct.*, **23**(4), 423-431.

Bouderba, B., Houari, M.S.A. and Tounsi, A. (2013), "Thermomechanical bending response of FGM thick plates resting on Winkler-Pasternak elastic foundations", *Steel Compos. Struct.*, **14**(1), 85-104.

Bourada, M., Kaci, A., Houari, M.S.A. and Tounsi, A. (2015), "A new simple shear and normal deformations theory for functionally graded beams", *Steel Compos. Struct.*, **18**(2), 409-423.

Buczkowski, R. and Torbacki, W. (2001), "Finite element modelling of thick plates on two-parameter elastic foundation", *Int. J. Numer. Analy. Method. Geomech.*, **25**(14), 1409-1427.

Chucheepsakul, S. and Chinnaboon, B. (2003), "Plates on two-parameter elastic foundations with nonlinear boundary conditions by the boundary element method", *Comput. Struct.*, **81**(30), 2739-2748.

Daouadji, T.H. and Tounsi, A. (2013), "Analytical solution for bending analysis of functionally graded plates", *Sci. Iranica*, **20**(3), 516-523.

Daouadji, T.H., Henni, A.H., Tounsi, A. and El Abbes, A.B. (2012), "A new hyperbolic shear deformation theory for bending analysis of functionally graded plates", *Model. Simul. Eng.*, **2012**, 29.

Hamidi, A., Houari, M.S.A., Mahmoud, S.R. and Tounsi, A. (2015), "A sinusoidal plate theory with 5-unknowns and stretching effect for thermomechanical bending of functionally graded sandwich plates", *Steel Compos. Struct.*, **18**(1), 235-253.

Liu, F.L. (2000), "Rectangular thick plates on Winkler foundation: differential quadrature element solution", *Int. J. Solid. Struct.*, **37**(12), 1743-1763.

Mahi, A. and Tounsi, A. (2015), "A new hyperbolic shear deformation theory for bending and free vibration analysis of isotropic, functionally graded, sandwich and laminated composite plates", *Appl. Math. Model.*, **39**(9), 2489-2508.

Meziane, M.A.A., Abdelaziz, H.H. and Tounsi, A. (2014), "An efficient and simple refined theory for buckling and free vibration of exponentially graded sandwich plates under various boundary conditions", *J. Sandwich Struct. Mater.*, **16**(3), 293-318.

Neves, A.M.A., Ferreira, A.J.M., Carrera, E., Cinefra, M., Roque, C.M.C., Jorge, R.M.N. and Soares, C.M.M. (2012), "A quasi-3D hyperbolic shear deformation theory for the static and free vibration analysis of functionally graded plates", *Compos. Struct.*, **94**(5), 1814-1825.

Patel, B.P., Ganapathi, M. and Makhecha, D.P. (2002), "Hygrothermal effects on the structural behaviour of thick composite laminates using higher-order theory", *Compos. Struct.*, **56**(1), 25-34.

Reddy, J.N. (2000), "Analysis of functionally graded plates", *Int. J. Numer. Method. Eng.*, **47**(1-3), 663-684.

Shen, H.S. (1999), "Nonlinear bending of Reissner-Mindlin plates with free edges under transverse and in-plane loads and resting on elastic foundations", *Int. J. Mech. Sci.*, **41**(7), 845-864.
Suresh, S. and Mortensen, A. (1998), "Fundamental of functionally graded materials", Maney, London.
Tanigawa, Y. (1995), "Some basic thermoelastic problems for nonhomogeneous structural materials", *Appl. Mech. Rev.*, **48**(6), 287-300.
Timoshenko, S.P. and Woinowsky-Krieger, S. (1959), "Theory of plates and shells", McGraw-Hill, New York.
Tlidji, Y., Daouadji, T.H., Hadji, L., Tounsi, A. and Bedia, E.A.A. (2014), "Elasticity solution for bending response of functionally graded sandwich plates under thermomechanical loading", *J. Therm. Stress.*, **37**(7), 852-869.
Tounsi, A., Houari, M.S.A. and Benyoucef, S. (2013), "A refined trigonometric shear deformation theory for thermoelastic bending of functionally graded sandwich plates", *Aerospace Sci. Tech.*, **24**(1), 209-220.
Tungikar, V.B. and Rao, K.M. (1994), "Three dimensional exact solution of thermal stresses in rectangular composite laminate", *Compos. Struct.*, **27**(4), 419-430.
Voyiadjis, G.Z. and Kattan, P.I. (1986), "Thick rectangular plates on an elastic foundation", *J. Eng. Mech.*, **112**(11), 1218-1240.
Wattanasakulpong, N., Prusty, B.G., Kelly, D.W. and Hoffman, M. (2012), "Free vibration analysis of layered functionally graded beams with experimental validation", *Mater. Des.*, **36**, 182-190.
Yahia, S.A., Atmane, H.A., Houari, M.S.A. and Tounsi, A. (2015), "Wave propagation in functionally graded plates with porosities using various higher-order shear deformation plate theories", *Struct. Eng. Mech.*, **53**(6), 1143-1165.
Zenkour, A.M. (2006), "Generalized shear deformation theory for bending analysis of functionally graded plates", *Appl. Math. Model.*, **30**(1), 67-84.
Zenkour, A.M. (2009), "The refined sinusoidal theory for FGM plates on elastic foundations", *Int. J. Mech. Sci.*, **51**(11), 869-880.
Zhu, J., Lai, Z., Yin, Z., Jeon, J. and Lee, S. (2001), "Fabrication of ZrO 2–NiCr functionally graded material by powder metallurgy", *Mater. Chem. Phys.*, **68**(1), 130-135.
Zidi, M., Tounsi, A., Houari, M.S.A. and Bég, O.A. (2014), "Bending analysis of FGM plates under hygro-thermo-mechanical loading using a four variable refined plate theory", *Aerospace Sci. Tech.*, **34**, 24-34.

*OP*